Look ahead dynamic security-constrained economic dispatch considering frequency stability and smart loads

Masoud Javadi[a], Turaj Amraee[a,*], Florin Capitanescu[b]

[a] Faculty of Electrical and Computer Engineering, K. N. Toosi University of Technology, Tehran, Iran
[b] Luxembourg Institute of Science and Technology (LIST), 4422 Belvaux, Luxembourg

ARTICLE INFO

ABSTRACT

Conventional economic dispatch models aim to determine the optimal production of generation units under the steady state operation constraints. Due to the growing integration of low inertia power generation technologies (e.g. wind, solar, etc.), considering stability constraints, in particular, frequency stability, a theme of this work, becomes a crucial need in nowadays security-constrained economic dispatch (SCED) programs. This paper develops a new look ahead dynamic (i.e. multi-period) security-constrained economic dispatch model, further considering frequency stability constraints (DSCED-FSC). The aim of the DSCED-FSC is to optimize the cost of power generation subject to operation and frequency stability constraints under normal and contingency conditions. The proposed DSCED-FSC secures N-1 contingencies for both thermal limits and frequency stability. The system frequency response is included in DSCED-FSC model by linearizing the discretized rotor angle swing equation. The dynamic models of governors and load damping are considered in the discretized system frequency response. The safety of system frequency response under generation outages is provided by activating generators' governors, inertial response and load damping as the primary frequency reserve. In addition to primary frequency reserve, the demand elasticity of smart motor loads is utilized to avoid the activation of under frequency load shedding (UFLS) relays under severe generation outages. The proposed DSCED-FSC model is formulated as a mixed integer linear programming (MILP) problem. The nonlinear AC power flow equations are linearized using Taylor series expansions and piecewise linear (PWL) approximation techniques. The efficacy of the proposed DSCED-FSC model in supporting system frequency is investigated using the IEEE 118-bus test system.

1. Introduction

1.1. Motivations and literature review

Economic and secure short term operation of power system is realized by solving sequentially, on daily basis, the security-constrained unit commitment (SCUC) [1] and, on hourly basis, the security-constrained economic dispatch (SCED) [2,3], the latter being a special case of security-constrained optimal power flow (SCOPF) [4]. This work focuses on SCED, which looks at minimizing the total cost of power generation to supply a given load demand while satisfying units and network constraints under both normal and contingency conditions. Furthermore, this work builds on the dynamic security constrained economic dispatch (DSCED) framework, which determines the optimal power production of the committed generating units over a given time interval [5,6]. The DED extends the conventional ED problem by

incorporating generator ramp rate constraints and time aspects.

Due to the growing integration of low inertia power generation technologies (e.g. wind, solar, etc.), considering stability constraints, in particular, frequency stability, a theme of this work, becomes a crucial need in nowadays SCED programs.

Frequency stability is the ability of a power system to maintain steady frequency following a severe contingency (e.g. large generator outage) resulting in imbalance between generation and load. When a loss of generation unit occurs, other available synchronous machines will release kinetic energy into the grid causing decline in their rotational speed and thereby system frequency, phenomenon referred to as inertial response. If system frequency drops below a pre-determined level or the rate-of-change-of-frequency (RoCoF) exceeds a predefined threshold, automatic under frequency load shedding (UFLS) and RoCoF relays are activated. UFLS relays are set to automatically disconnect a certain amount of load in few subsequent stages whenever frequency

Nomenclature

Indices

n	Index of time steps in frequency response
i, j	Index of buses
m	Index of smart load types
t	Index of time
l/k	Index of piecewise segments in the linearized fuel cost function/AC power flow model
$\{\bullet\}^{min/max}$	Minimum/maximum of a given variable

Sets and parameters

Ω_B/N_B	Set/number of all buses
Ω_G/N_G	Set/number of all generation nodes
Ω_L/N_L	Set/number of all load buses
Ω_{TL}/N_{TL}	Set/number of all transmission lines
Ω_T	Set of periods in study horizon
T	Duration of multi-period study
N_{SF}/N_{SC}	Number of segments for linearized cost function/cosine function
N_{LT}	Number of load types
f_0/f_{ss}	Nominal/steady state frequency of the system
f_{min}	Minimum allowable frequency of the system
f_i^{dr}	Operating drive/minimum allowable frequency of smart load type m
f_i^{dr-min}	Minimum allowable operating drive frequency of smart load located at bus i
k_f	Smart motor load parameter representing frequency-dependency of active power load
RU/RD	Ramp up/down limits of thermal units
$LE_{i,m}^{max}$	Maximum amount of load reduction by smart load type m at bus i

Δt	Time step in discretized frequency response
Δt_r	Time step for ROCOF calculation
H/H^*	Inertia constant of generator/entire system
D	Load damping factor
R/R^*	Governor droop at base MVA of generator/entire system
T_g/T_s	Time constant of governor/smart load
G/B	Network conductance/susceptance matrix

Variables

$f_n/\Delta f_n$	Frequency/frequency deviation at time step n
f_{nadir}	Minimum post contingency frequency value
$\Delta P_{n,m}^{SL}$	Smart load reduction type m at time step n
ΔP_n^{Gov}	Governor response at time step n
ΔP^c	Generation outage under contingency
P_d/Q_d	Active/reactive load demand
P_g/Q_g	Active/reactive power generation
p_g^l	Power generation of lth linear segment
RS	Reserve for primary frequency control
$v\angle\delta$	Voltage phasor
η_l	Slope of lth segment in linear cost function
$\hat{\delta}/\tilde{\delta}$	Voltage angle/positive angle approximation
S_k	Slope of kth segment located in positive argument of cosine function
$\tilde{d}_k$	Value of kth segment of positive voltage angle approximation
y	Approximation of cosine function
W	Binary decision variable indicating the sign of voltage angle difference
$\tilde{U}_k$	Binary decision variable for k^{th} segment of positive voltage angle approximation
XP, XN	Auxiliary variables

falls below a threshold [7,8]. Also, RoCoF relays (i.e. as the anti-islanding protective relays of synchronous distributed generators) under abnormal RoCoF values will disconnect the small scale synchronous generators in the distribution system. The power system must be able to survive all single generating outages without the activation of these two relays.

The primary frequency control (PFC), the focus of this work, includes the inertial response, governor action, and load damping. PFC is an automatic feedback control that adjusts the mechanical power of the generators equipped with speed governor to stabilize the frequency declines following large generation outages. The timescale of this control is up to tens of seconds (e.g. 20–30 sec from the beginning of the generation outage). Secondary frequency control is a centralized automatic control that adjusts the active power production of the generating units to restore the frequency and the interchanges with other areas to their target values following a power imbalance. In other words, while the primary frequency control limits and stops the frequency excursions, the secondary frequency control brings the area control error (ACE) back to zero (i.e. brings the frequency back to its target value). Tertiary frequency control refers to the manual changes in the dispatching and commitment schedule of generating units. This control is used to restore the primary and secondary frequency control reserves, to manage congestions in the transmission network, and to bring the frequency back to its nominal value when the secondary control is unable to do so [9]. The secondary and tertiary frequency controls are outside the scope of this paper.

Various approaches have been proposed to address the frequency stability problem, with the help of new technologies and devices such as energy storage systems (ESS) [10,11], synthetic or virtual inertia from variable-speed wind turbines [12], and the fast frequency response reserve from loads [13]. Due to the growth of renewable penetration and operation of generators near to their maximum output during heavy loading conditions, the use of demand-side management (DSM) options has attracted much interest [14]. PFC via the demand response (DR) is a relatively new concept in smart grids which may be accomplished using advanced power electronics and communication technologies. Various types of thermoelectric controllable loads such as electric heating systems, refrigerators, freezers, and air conditioners have great potential to provide primary frequency response, inasmuch as they account for a considerable portion of the total load demand [15,16]. This type of control can be achieved through either ON/OFF commands or power electronics controllers. The latter is a continuous controller that acts like a governor with a droop characteristic [17]. In [18], a droop control is used to model EV and electric water heater load clusters for primary and secondary frequency control in a multi-agent power system. In [19], Light-Emitting Diode (LED) lighting loads are introduced as another efficient source of frequency control source providing a flexible load demand with low impact on users' comfort level. According to the frequency control scheme proposed in [19], the frequency deviation is responded by the change in the illumination of LED lighting loads according to its magnitude and duration to provide frequency regulation. Utilizing the frequency-supporting advantages of smart loads under credible outages in ED study has not been addressed in previous researches. However, smart loads can be employed to preserve the frequency stability under generation outages so as to avoid intentional activation of UFLS relays.

While transient and voltage stability constraints inclusion in SCOPF have been explored for more than one decade [4], recently, there has

been significant interest in incorporating frequency response into various operational and planning studies of power systems. In [20], a UC formulation is developed considering the adequacy of reserves for primary and tertiary frequency control. The primary frequency reserve provision of generating units is modeled neglecting the transient frequency response that may activate UFLS relays. In [21], a set of constraints on the system inertia is proposed to control Rate-of-Change-of-Frequency (RoCoF) during high penetration of non-synchronous penetration level. In [22], a UC model is developed respecting frequency limits using DC power flow model and without considering the post-contingency conditions and load damping effect. In [23], a SCUC model with linearized frequency constraints has been proposed. The nonlinear minimum frequency function is linearized using a piecewise linear (PWL) technique and power balance is provided using DC power flow model. In [24], frequency stability constraints have been considered in the optimal power flow (OPF) problem to ensure the adequacy of primary frequency response without considering the impacts of the load damping. Ref. [25] develops a stochastic ED formulation with frequency stability constraints under wind uncertainty. In [26], a real-time MILP-based islanding protection scheme is developed considering frequency stability assuming a simple approximation of AC power flow equations. In [27], primary frequency response constraints are used in the generation and storage capacity expansion study. However, the dynamics of frequency response and consideration of frequency nadir is neglected. Recently, a frequency stability constrained economic dispatch model has been proposed in [28], which approximates frequency nadir through cutting planes technique. However, the details of the considered operation and security constraints along with the accuracy of the proposed method have not been developed. Frequency stability constraints have been also used in the optimization-based UFLS studies such as [7,29]. As discussed, the previous studies have shortcomings such as inaccurate approximation of the system frequency response, utilization of DC power flow model, and neglecting the security of the system (i.e. post-contingency conditions). The present paper attempts to overcome the aforementioned drawbacks, providing a more realistic and accurate model of the frequency stability constraints in an MILP-based DED scheme. A comparison of relevant previous works is provided in Table 1.

The focus of this paper is not to show the difference between AC-OPF and DC-OPF problems, particularly for frequency stability purposes. The pros and cons of AC-OPF and DC-OPF have been discussed in previous researches such as [30]. Indeed, AC-based models have some advantages over the DC-based models: a) they consider voltage and reactive power aspects b) they implicitly model the active power losses. On the other hand, while DC models may lead to infeasible solutions, AC-OPF models are non-convex and hence the global optimum may not always be obtained. In this paper, we use a linearized AC model which

we have proven better accuracy than DC model regarding the transmission network constraints. The allocation of spinning reserve to support frequency stability under given generation contingencies depends not only primarily on frequency stability constraints but also on the transmission network constraints because the activation of this reserve must not violate branch thermal limits (and create congestion) or bus voltage limits. Therefore, not only the overall amount but also the allocation of spinning reserves between generators are essential. For these reasons, it is important to model as accurately as possible branches thermal limits, bus voltage limits, and generators reactive power limits to support the voltage limits. And, as proven by our previous works in [31,32], our linearized AC model is more accurate than the DC model and hence more suitable for this task. Hence, using the DC power flow, the obtained results might be unrealistic and underestimated.

1.2. Contributions

This paper expands the DED models existing in the literature [5,6] with original contributions such as: (i) contingency constraints (both static, i.e. thermal line limits, and dynamic, i.e. frequency stability constraints including smart loads participation) and (ii) proposing a look-ahead (i.e. multi-period) DSCED under frequency stability constraints (DSCED-FSC), which is formulated as an MILP. Our approach also extends the classical SCED [2] in terms of look ahead (dynamic or multi-period) aspect, frequency stability constraints considering also smart loads.

1.3. Paper organization

The remaining of this paper is organized as follows. Section 2 presents the detailed model of primary frequency response. The formulation of the proposed DSCED-FSC model is described in Section 3. The simulation results of the developed model using the IEEE 118-bus test system are presented in Section 4. Finally, Section 5 concludes.

2. Dynamic model of primary frequency response

This section develops the primary frequency response dynamic model, which allows deriving frequency stability constraints (both on frequency absolute value and RoCoF) to be included in the proposed DSCED-FSC model.

The different strategies that can be used to stabilize the post-contingency frequency response are shown in Fig. 1. Under the credible generation outage, to avoid the activation of UFLS relays, the nadir of system frequency response must be greater than a minimum allowable threshold in all circumstances. The frequency set-point of the first stage of some of the practical UFLS schemes around the world is given in

Table 1
Comparison of notable previous works.

| Ref	Study/objective function	Constraints
[20]	UC/minimization of total cost of generation and tertiary and primary reserve service	Lossless network model, operational limits, reserve limits to control steady-state system frequency
[22]	UC/minimization of total cost of generation and reserve and cost of batteries' operation	DC power flow model, operational constraints, RoCoF, and frequency nadir limits
[23]	UC/minimization of total generation cost	DC power flow model, operational limits, frequency nadir constraint
[24]	OPF/minimization of total generation and reserve cost	Lossless network model, operational limits, constraints of adequacy of primary frequency response
[25]	Stochastic ED/minimization of expected generation and reserve costs + Minimization of cost of generation redispatch and unserved load	Lossless network model, operational and reserve limits, security constraints of transmission lines, load shedding constraints, etc
[26]	Controlled islanding/minimization of total amount of load shedding	Simplified AC power flow model, operational limits, constraints on frequency nadir, frequency overshoot, and steady-state frequency, etc
[27]	Generation capacity expansion/minimization of investment cost of generating and storage units, expected cost of operation of generating units and load shedding	DC power flow model, operational limits, constraints of frequency deviation from nominal value, etc.
[7]	Under frequency load shedding/minimization of total amount of load shedding	Frequency stability constraints such as RoCoF, frequency nadir, steady-state frequency, etc.
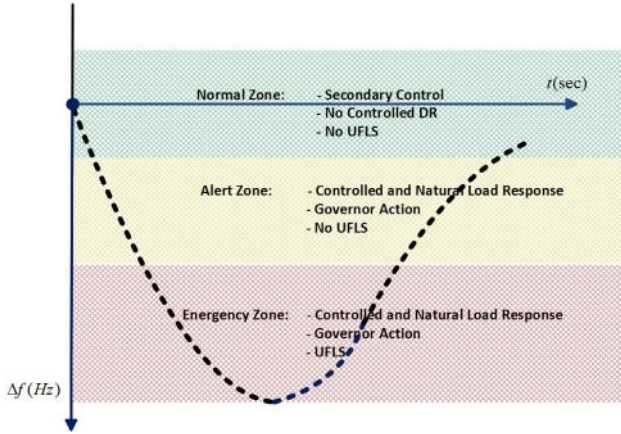
Fig. 1. Hierarchy of primary frequency measures.

Table 2
Frequency set-point of the first stage of the UFLS schemes implemented by different entities [7,33].

Entity	f_{min}
Ireland ESB	48.5
Nordel	48.8
Iran national grid	49.4
Western Electricity Coordinating Council (WECC) (60 Hz)	59.1
Electric Reliability Council of Texas (ERCOT), Mid Continent Area Power Pool (MAPP), Southwest Power Pool (SPP), Mid America Interconnected Network (MAIN), Mid Atlantic Area Council (MAAC), Northwest Power Pool (NWPP), Northeast Power Coordinating Council (NPCC) (60 Hz)	59.3
East Central Area Reliability coordination agreement (ECAR) (60 Hz)	59.5
Florida Reliability Coordinating Council (FRCC) (60 Hz)	59.7

Table 2. As depicted in Fig. 1, this frequency is the threshold of the emergency zone.

As shown in Fig. 1, all frequency deviations inside a safe range (i.e. $\pm 0.5Hz$ according to [33] as shown in green in Fig. 1), can be normalized using secondary frequency control (i.e. via Automatic Generation Control (AGC)). Under severe generation outages, (e.g. credible double or higher order generation outages), the frequency deviations may exceed the safe range. In these conditions (i.e. Alert or Emergency zones as shown in Fig. 1), the focus of this paper is to utilize the sources of primary frequency control to restore the frequency to the safe range. In alert zone, the load elasticity is utilized unlike the emergency zone in which both load elasticity and load shedding are allowed. Also, it is assumed that the primary frequency reserve is deployed in response to frequency deviations caused only by generation outages and not those deviations caused by load perturbations (i.e. non-contingent perturbations). Traditionally severe frequency deviations are compensated by governor actions and UFLS activations along with the natural inertial response and load damping. According to Fig. 1, in this paper, the elasticity of non-critical smart loads is utilized to postpone or even avoid the load shedding under such conditions. Non-critical loads (i.e. loads with low priority and a high power rating that have minimal impact on comfort levels of customers such as electric water heaters, refrigerators, heating, ventilating and air-conditioning (HVAC), and motor loads [34,35]) are static or dynamic loads that can tolerate the voltage and frequency excursions for a short time. The block diagram of the proposed frequency response model has been depicted in Fig. 2.

The swing equation of a multi-machine power system can be approximated based on the center of inertia (COI) concept [36]. The frequency response of the system is governed by the swing equation as given in (1)–(3):

$$\frac{d\Delta f(t)}{dt} = \frac{1}{2H^*}\left[-\Delta P^c + \sum_{i=1}^{N_G} \Delta P_i^{gov}(t) + \sum_{m=1}^{N_{Ty}}\sum_{i=1}^{N_L} \Delta P_{i,m}^{SL}(t) - D\Delta f(t)\right] \quad (1)$$

$$\frac{d\Delta P_i^{gov}(t)}{dt} = \frac{1}{T_{gi}}\left(-\Delta P_i^{gov}(t) - \frac{\Delta f(t)}{R_i^*}\right) \quad (2)$$

$$R_i^* = \frac{R_i S_B}{S_i}, \quad H^* = \sum_{i=1}^{N_G}\frac{H_i S_i}{S_B}, \quad S_B = \sum_{i=1}^{N_G} S_i \quad (3)$$

The system frequency response governed by (1) is considered as the constraint of DSCED under generation outage of ΔP^c. The amount of ΔP^c is assumed to be equal to the largest generating unit of the contingencies set. Using Euler's method [37], the system frequency and the dynamic response of generation and demand side resources can be discretized into time steps with duration of Δt, as follows:

$$\Delta f_n = \Delta f_{n-1} + K_{n-1}\Delta t \quad (4)$$

$$K_n = \frac{1}{2H^*}\left(-\Delta P^c + \sum_{i=1}^{N_G} \Delta P_{n,i}^{gov} + \sum_{m=1}^{N_{Ty}}\sum_{i=1}^{N_L} \Delta P_{n,i,m}^{SL} - D\Delta f_n\right) \quad (5)$$

$$\Delta P_{n,i}^{gov} = \Delta P_{n-1,i}^{gov} + \frac{\Delta t}{T_{gi}}\left(-\frac{\Delta f_{n-1}}{R_i^*} - \Delta P_{n-1,i}^{gov}\right) \quad (6)$$

Similar to the primary frequency reserve provided from inertial or governor response, the load demand may provide two responses including the natural response caused by load damping of motor loads, and controlled response provided by smart loads. The latter provides load elasticity in response to the change of frequency without any centralized controller. Note that the aim of the Power System Stabilizer (PSS) and Automatic Voltage Regulator (AVR) is to ensure the small signal stability and transient stability, respectively and their time response is very rapid with respect to the time constant of the frequency stability. In this regard, during frequency stability studies it is assumed that the dynamics of PSS and AVRs have been died out and the system has survived dynamically this transitory period [36].

Traditionally, the frequency dependency of inductive motor loads has been considered in load frequency control of the power system, and this is called the natural load response considered by the load damping factor. However, in smart loads, the amount of consumption is intentionally controlled in response to the change of system frequency. Unlike the natural load response, in smart loads, there is additional equipment to control the amount of load under severe changes in system frequency. Such response can be provided by different loads such as motor-drive loads and thermostatic loads using local frequency measurements obtained by a smart meter [38]. For instance, the flexibility of the high and low temperature setpoints of the thermostatically
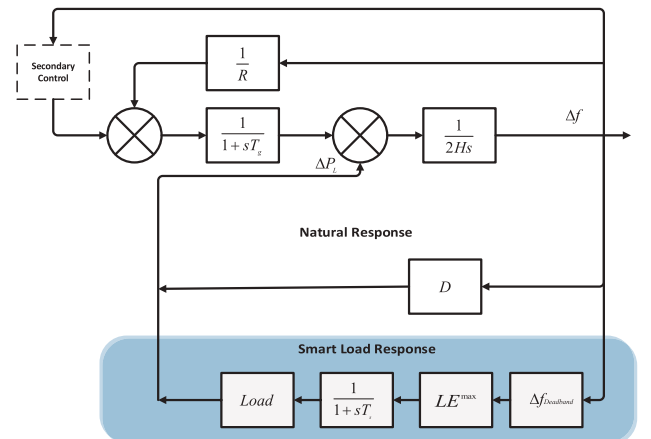

Fig. 2. Block diagram of the proposed system frequency response.

controlled loads (TCLs) such as electric water heaters and HVACs can be utilized to provide a substantial frequency reserve while this does not affect the comfort level of the consumers in the short time horizon of PFC [35]. The flexibility of smart loads is generally dependent on several factors such as interruptibility, time of use, priority defined by the users, behavior of the consumers [39,40]. Indeed, smart loads are non-critical loads which depending on the measured quantity (e.g. frequency or voltage) their demand can be controlled through a controller. A general framework of smart loads is depicted in Fig. 3. Different types of smart load including static (i.e. voltage dependent) or dynamic (i.e. frequency dependent) loads may be included in system frequency response. The details of possible controllers for smart loads can be found in [16]. In order to control a static voltage dependent smart load, it is needed to implement an additional power electronic device to control the input voltage of the loads. However, the smart motor loads with their own variable frequency drives do not incur additional cost. In this regard, the elasticity of induction motors controlled by variable frequency drives is utilized as the smart load to soften severe system frequency declines.

The smart load model proposed in (7)–(8) deploys the maximum load elasticity (i.e. primary reserve of the smart load) within a given time constant. As given in (8), the maximum possible primary reserve by the smart motor load depends on operating frequency of the motor at the time of contingency (i.e. $f_{i,m}^{dr}$), the minimum possible frequency of the drive (i.e. $f_{i,m}^{dr-min}$) and the frequency sensitivity of the load type (i.e. k_{f-m}). As discussed in [16], the operating drive frequency is a random parameter. The related smart motor load cannot participate in primary frequency control immediately but only after a time delay in a dynamic regime as given in (7). Indeed, the variable of $LE_{i,m}^{max}$ in (8) gives the maximum power reserve by the smart motor loads. In other words, this reserve is provided by reduction of the operating frequency from $f_{i,m}^{dr}$ to $f_{i,m}^{dr-min}$.

$$\Delta P_{n,i,m}^{SL} = \Delta P_{n-1,i,m}^{SL} + \frac{\Delta t}{T_s}(LE_{i,m}^{max} - \Delta P_{n-1,i,m}^{SL})$$
(7)

$$LE_{i,m}^{max} = P_{0-i,m}\left[\left(\frac{f_{i,m}^{dr}}{f_0}\right)^{k_{f-m}} - \left(\frac{f_{i,m}^{dr-min}}{f_0}\right)^{k_{f-m}}\right]$$
(8)

The frequency of the system at the COI reference is calculated as follows:

$$f_n = f_0 + f_0\Delta f_n$$
(9)

To avoid the system frequency falling below a certain threshold and thus preventing the activation of under-frequency relays, the frequency response is not allowed to exceed a minimum value.

$$f_{nadir} \geq f_{nadir}^{min}$$
(10)

In addition to the frequency value, the amount of RoCoF should be constrained. To this end, the RoCoF value of the system frequency response must not exceed a predetermined threshold. The RoCoF value is calculated over a time window. The length of time window must be selected long enough to diminish the possible noise and errors.

The average RoCoF value over a measuring window (e.g. $N_{cy} = 10$ cycles or 200 ms in 50 Hz) is constrained at the end of related time window as given by (11)–(12).

$$RoCoF_n \leq RoCoF^{max}$$
(11)

$$RoCoF = \frac{df}{dt} \cong \frac{1}{N_{cy}}\sum_{i=1}^{N_c}\left(\frac{\Delta f_i}{\Delta t_r}\right)$$
(12)

Finally, the steady-state value of system frequency must remain within a safe range:

$$f_0 - \Delta f_{ss}^{max} \leq f_{ss} \leq f_0 + \Delta f_{ss}^{max}$$
(13)

The linear and discretized system frequency response including

different sources of primary frequency reserve, developed so far, will be included as major constraints in the DSCED model described hereafter.

3. Linearized DSCED-FSC model

The goal of the DSCED-FSC model is to minimize the cost of active power production of committed generating units over a given time horizon. Also, the proposed model may be used for minimizing the cost of active power deviations from their scheduled values (i.e. schedule obtained by a SCOPF or SCED without frequency stability constraints) to satisfy the frequency stability constraints. The objective function of the DSCED is expressed as follows:

$$Min \sum_{t=1}^{T}\sum_{i=1}^{N_G}\left(a_i(P_{gi}^t)^2 + b_iP_{gi}^t + c_i\right)$$
(14)

A PWL technique is utilized to linearize the quadratic cost function given by (14). Using the method described in [41], the linear equivalents of (14) are expressed as follows.

$$C_i^t(P_{gi}^t) = C_i^t(P_{gi}^{min}) + \sum_{l=1}^{N_{SF}}r_i^l p_{gi}^{l,t}$$
(15)

$$P_{gi}^t = P_{gi}^{min} + \sum_{l}^{N_{SF}}p_{gi}^{l,t}$$
(16)

$$0 \leq p_{gi}^{l,t} \leq \frac{P_{gi}^{max} - P_{gi}^{min}}{N_{SF}}$$
(17)

Besides the frequency stability constraints (4)-(13), the proposed model contains the constraints detailed hereafter. Unlike the DC power balance model, the linear AC power flow formulation approximates the line flows, voltage magnitudes, and reactive power generation with reasonable accuracy. The nonlinear AC power flow equations are linearized in (18)-(30) using Taylor series expansion around the normal operating point (i.e. $v = 1^{pu}$, $\delta_{ij}^t = 0$) using PWL technique [32].

$$(P_{gi}^t - P_{di}^t) = \sum_{j=1}^{N_B}(G_{ij}(v_i^t + v_j^t + y_{ij}^t - 2) + B_{ij}\hat{\delta}_{ij}^t)$$
(18)

$$(Q_{gi}^t - Q_{di}^t) = \sum_{j=1}^{N_B}\left(G_{ij}\hat{\delta}_{ij}^t - B_{ij}\left(v_i^t + v_j^t + y_{ij}^t - 2\right)\right)$$
(19)

where y_{ij}^t is the approximation of $\cos(\delta_{ij}^t)$ using N_{SC} linear segments. Due to the symmetry of cosine function (i.e. $\cos(-\delta) = \cos(\delta)$), a binary variable (i.e. W_{ij}^t) is defined to determine the sign of voltage angle difference, where $W_{ij}^t = 1$ corresponds to the positive sign and $W_{ij}^t = 0$ corresponds to the negative sign as given in (20).

$$\hat{\delta}_{ij}^t = W_{ij}^t\tilde{\delta}_{ij}^t - (1 - W_{ij}^t)\tilde{\delta}_{ij}^t$$
(20)

According to (21), the variable $\tilde{\delta}_{ij}^t$ (i.e. magnitude of voltage angle difference) is divided into $\frac{N_{SC}}{2}$ segments.

$$\tilde{\delta}_{ij}^t = \sum_{k=1}^{\frac{N_{SC}}{2}}\tilde{d}_{ij,k}^t$$
(21)

Due to the priority considered in this technique, a segment takes on value if and only if all its prior segments reach their upper bounds. Each
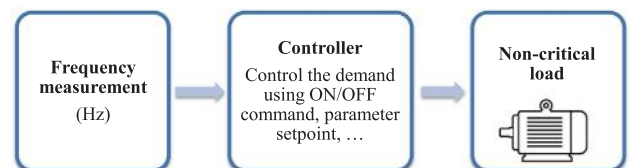

Fig. 3. The general framework of smart load.

segment is activated using another binary variable (i.e. $\widetilde{U}_{ij,k}^{t}$) as follows:

$$L_k \widetilde{U}_{ij,k+1}^{t} \leq \widetilde{d}_{ij,k}^{t} \leq L_k \widetilde{U}_{ij,k}^{t} \tag{22}$$

where L_k is the upper bound of kth segment.

The constraints given in (23)-(27) represent the linear equivalents of the nonlinear constraint (20). Finally, the cosine term is linearized as given in (28).

$$\widehat{\delta}_{ij}^{t} = XP_{ij}^{t} - XN_{ij}^{t} \tag{23}$$

$$0 \leq XP_{ij}^{t} \leq W_{ij}^{t} \tag{24}$$

$$\widetilde{\delta}_{ij}^{t} - (1 - W_{ij}^{t}) \leq XP_{ij}^{t} \leq \widetilde{\delta}_{ij}^{t} \tag{25}$$

$$0 \leq XN_{ij}^{t} \leq 1 - W_{ij}^{t} \tag{26}$$

$$\widetilde{\delta}_{ij}^{t} - W_{ij}^{t} \leq XN_{ij}^{t} \leq \widetilde{\delta}_{ij}^{t} \tag{27}$$

$$y_{ij}^{t} = 1 + \sum_{k=1}^{\frac{N_{SC}}{2}} S_k \widetilde{d}_{ij,k}^{t} \tag{28}$$

Based on the aforementioned linearized power flow model, the thermal limits of transmission lines are expressed and enforced as given in (29)-(31).

$$P_{L,ij}^{t} = G_{ij}(v_i^t + v_j^t + y_{ij}^t - 2) + B_{ij}\widehat{\delta}_{ij}^{t} - G_{ij}(2v_i^t - 1)(ij \in \Omega_{TL}, t \in \Omega_T) \tag{29}$$

$$Q_{L,ij}^{t} = G_{ij}\widehat{\delta}_{ij}^{t} - B_{ij}(v_i^t + v_j^t + y_{ij}^t - 2) + B_{ij}(2v_i^t - 1)(ij \in \Omega_{TL}, t \in \Omega_T) \tag{30}$$

$$-P_{L,ij}^{max} \leq P_{L,ij}^{t} \leq P_{L,ij}^{max}(ij \in \Omega_{TL}, t \in \Omega_T) \tag{31}$$

The operational limits of voltage magnitudes, reactive power of synchronous generators, active power generations, and spinning reserve for primary frequency control are expressed as given in (32)-(35), respectively:

$$v_i^{min} \leq v_i^t \leq v_i^{max}(i \in \Omega_B, t \in \Omega_T) \tag{32}$$

$$(Q_{gi}^{min}, Q_{ci}^{min}) \leq (Q_{gi}^t, Q_{ci}^t) \leq (Q_{gi}^{max}, Q_{ci}^{max})$$
$$(i \in \Omega_G, t \in \Omega_T) \tag{33}$$

$$P_{gi}^{min} \leq P_{gi}^t \leq P_{gi}^{max}(i \in \Omega_G, t \in \Omega_T) \tag{34}$$

$$0 \leq RS_i^t \leq P_{gi}^{max} - P_{gi}^t(i \in \Omega_G, t \in \Omega_T) \tag{35}$$

The ramp-up and ramp-down limits of generating units are considered using (36)-(37).

$$P_{gi}^t - P_{gi}^{t-1} \leq RU_i(i \in \Omega_G, t \in \Omega_T) \tag{36}$$

$$P_{gi}^{t-1} - P_{gi}^t \leq RD_i(i \in \Omega_G, t \in \Omega_T) \tag{37}$$

Note that, albeit not shown explicitly, the operational and the frequency stability constraints must be satisfied for a set of postulated credible N-1 contingencies for each time period. The general framework of the proposed DSCED-FSC model is shown in Fig. 4.

4. Simulation results

The IEEE 118-bus test system is used to evaluate the efficiency of the proposed DSCED-FSC model. The IEEE 118-bus test system has 54 generating units, 14 capacitors, 186 branches, and peak load of 3733 MW. The static data of this test system can be found in [1]. For the sake of illustration and results reproducibility, a look ahead horizon of 6 time periods is considered, corresponding e.g. to 6-hour ahead time horizon (from hour 8 to hour 13 as committed according to [1]) is considered for simulations. It is assumed that the hourly commitment of generating units has been determined in prior. We assume a set of 5/23N-1 line/generator contingencies.

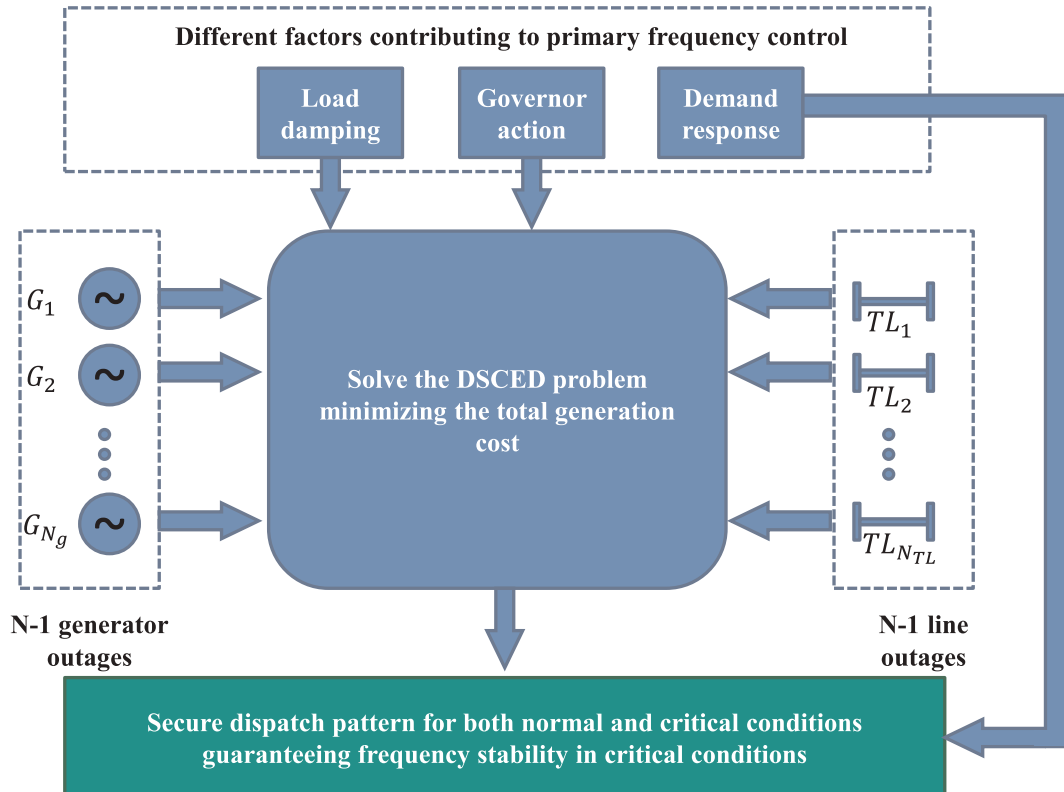The required data for modeling the system frequency response have

Fig. 4. A schematic overview of the proposed DSCED-FSC method.

Table 3
Parameters of smart frequency-responsive motor loads.

Load type	Share of responsive motor loads (%)	k_f
Space heating	34	2.66
Industrial large motor	15	2.99
Industrial small motor	20	2.98
HVAC	20	2.66
Compressor	11	2.99

been collected from [42]. The generating units supposed to participate in primary frequency control by governor action are G4, G11, G21, G27, G28, G36, G39, G40, and G43. The nominal frequency of the system is 50 Hz. The load damping factor is assumed to be equal to 1 (i.e. 1% change in system frequency results in 1% change in load demand). The time step of the discretized frequency response model is set to 100 ms and the response is simulated for 30 s. The proposed MILP models are solved using the Gurobi solver [43] in GAMS [44]. The specifications of the considered responsive smart loads are presented in Table 3. The minimum allowable frequency of the drive is assumed to be 30 Hz. Moreover, it is assumed that responsive drive-connected smart motor loads constitute 7.5% of the total load. The time constant of these smart loads is assumed to be 0.5 s. It should be noted that, in the figures, the time t = 0 sec corresponds to the generation outage.

4.1. Case study I: Conventional DSCED

The conventional DSCED model is solved without considering the frequency stability constraints. The generation output results are reported in Table 4. It is assumed that the spinning reserve must be greater than the largest generating unit. The total cost of power generation over the time horizon is 226480.77$. The system frequency deviations under all single generator outages have been depicted in Fig. 5. The settings of multistage UFLS relays in different countries can be found in [33]. According to [33], different thresholds may be set for the first stage of UFLS relays.

According to [33], practically, three to five UFLS plans are utilized by the various entities. The range for the first load shed step is a decay of 0.3 Hz to 0.9 Hz and the subsequent stages range from 0.2 Hz to

0.5 Hz with load percentages varying from 5% to 15% system load per stage. Assuming the minimum allowable frequency nadir as 49.4 Hz, a 4-step UFLS as 49.4 Hz, 49.2 Hz, 49.00 Hz, and 48.8 Hz with 10%, 10%, 10%, and 10% load shed blocks is assumed. Using the proposed DSCED-FSC, the activation of early stages of UFLS relays may be avoided by utilizing the governors and smart loads. As depicted in Fig. 5, one of these outages (i.e. outage of G36 at hours 8–13) causes the frequency to exceed the minimum allowable frequency nadir. The minimum value of the frequency nadir is 49.11 Hz, following the sudden outage of G36 at hour 8. According to Fig. 5, following the outage of G36, the frequency deviation is 0.8865 Hz, 0.7925 Hz, 0.8247 Hz, and 0.7052 Hz at hours 8, 9, 10, and 11–13, respectively. It can be seen that following the outage of G36, the minimum allowable frequency has been violated in all time periods. It can be seen that the conventional dispatch will not fulfill the system frequency stability constraints and the first stage of UFLS relays will be activated (leading to a load shedding of 256.34 MW or 10% system load), which fully justifies our proposed approach to secure operation against loss of load and frequency instability.

4.2. Case study II: DSCED-FSC model

In this case, the optimal power generations and related spinning reserves are determined considering the frequency stability constraints. The results of generation re-dispatch to satisfy the frequency stability constraints under generation outages have been highlighted in Table 4. The system frequency deviations from their nominal value under all single generating outages have been illustrated in Fig. 6. It can be seen that by considering the frequency stability constraints including the governor actions, the system frequency under all single generating outages, remains within its predefined safe range, avoiding load shedding (i.e. 10% of load is saved). The dynamics of the active power generation of responsive generators under the most severe contingency (i.e. outage of G36) at the peak hour is depicted in Fig. 7. According to Fig. 7, the post-contingency active power generation of synchronous generators are within their allowable range. Furthermore, as depicted in Fig. 8, by utilization of the smart motor loads in the demand side, the frequency nadir reaches 49.7 Hz at the peak hour, which is far from the threshold of the first stage of UFLS relays. Assuming the UFLS settings as considered in Case I, the first stage set-point of the UFLS relays is as 49.4 Hz and 10% load shed. Under N-2 contingencies, it can be seen

Table 4
Generation schedule of the proposed DSCED-FSC problem either considering frequency constraints (case II) or not (case I).

| Gen. No.	t=8		t=9		t=10		t=11,13		t=12	
	Case I	Case II	Case I	Case II	Case I	Case II	Case I	Case II	Case I	Case II
4	202.5	202.5	207.66	220	223.43	237.5	237.5	237.5	237.5	238.85
5	160	160	170	180	190	200	201.13	203.96	208.52	210
10	170	178.88	180	190	200	210	210	210	210	211.16
11	200	200	212.5	212.5	228.95	237.5	237.5	237.5	237.5	237.5
20	120	130	120	130	145.75	150	150	150	150	159.41
21	0	0	90	90	110	110	110	120	110	120
24	0	0	80	87.5	95	105.23	102.5	110	102.5	110
25	0	0	72.5	80	87.5	95.41	95	99.62	95	102.5
27	164	180	164	164	180	196	180	196	196	196
28	108.08	124.30	116	116	132	148	132	148	134.89	148
29	278	289	278	289	300	300	300	300	300	300
30	80	80	80	80	80	80	80	80	80	80
34	96.25	100	100	100	100	100	100	100	100	100
35	100	100	100	100	100	100	100	100	100	100
36	412.5	279.18	430	325.56	447.5	325.56	447.5	380.73	447.5	380.73
37	88.75	100	100	100	100	100	76.61	74.25	76.45	74.99
39	0	0	0	0	0	0	200	200	200	200
40	220	237.5	237.5	241.65	255	259.64	237.5	238.27	236.79	237.5
43	130	148.89	140	150	156.01	170	131.18	140	140	140
45	190	210	200	210	220	230	210	210	210	220
51	0	0	52.09	62.5	82.09	76.18	62.5	63.32	66.25	70.23
53	100	100	100	100	100	100	100	100	100	100
54	50	50	50	50	50	50	50	50	50	50
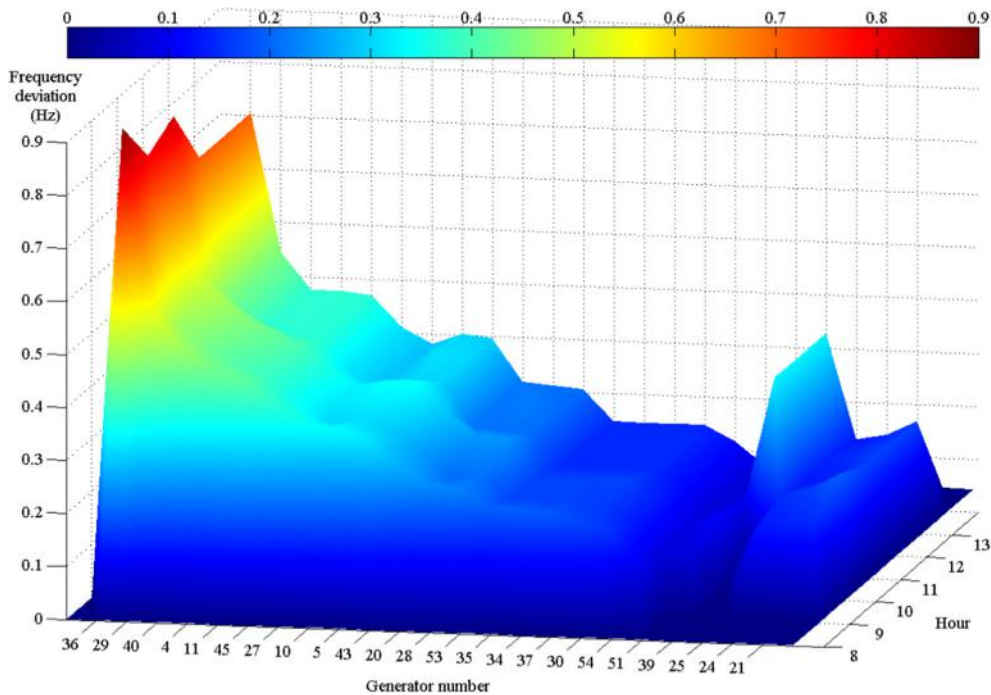
Fig. 5. Frequency deviations of different contingencies (i.e. generation outages) at each interval (i.e. hour) in case I.
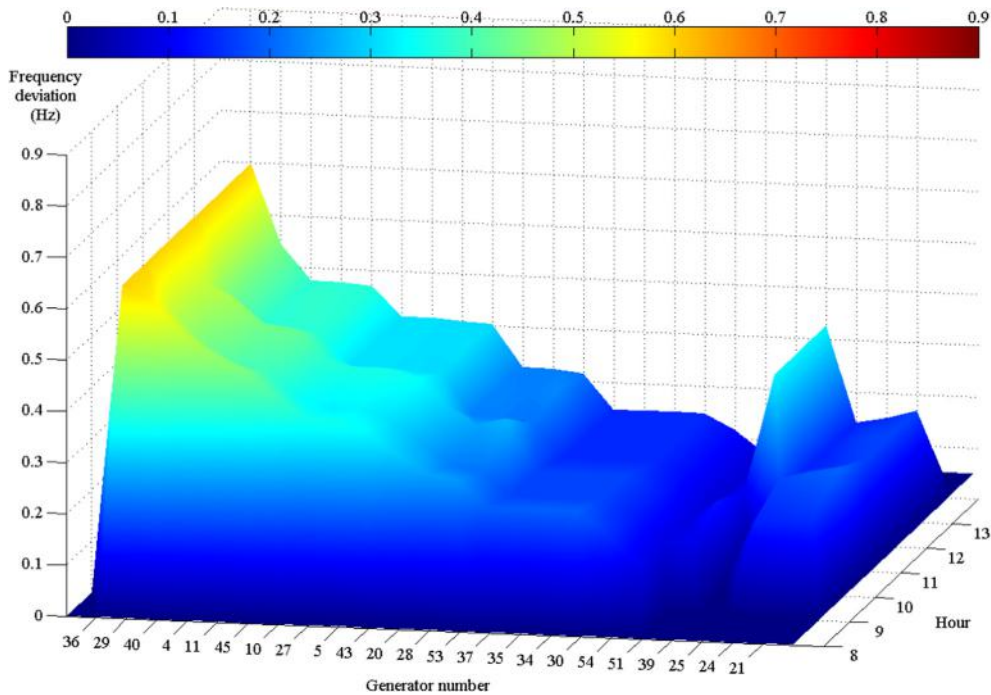

Fig. 6. Frequency deviations of different contingencies (i.e. generation outages) at each interval (i.e. hour) in case II.

that without the smart load (only using the generation re-dispatch and governor actions) the frequency nadir is 49.27 and the considered UFLS plan shed 337.3 MW (i.e. 10% of system load) while by using 206.19 MW elasticity from smart loads, such amount of load shedding is avoided. Additionally, using the smart loads, the load reduction is achieved without disconnecting or shedding the load from the grid. Furthermore, the smart load raises the frequency nadir and steady state system frequency more than the UFLS scheme.

In this case, the total cost of generation has been slightly increased by 0.27% (i.e. 227097.90$) to ensure the system frequency stability.

The simulation results indicate that the proposed method ensures

that the frequency nadir does not exceed the acceptable system frequency limits under credible generation outages.

4.3. Case study III: Impact of non-synchronous generations

Growing penetration of inverter-based non-synchronous generations (e.g. wind or photovoltaic) has resulted in decrease in the system inertial response, due to the fact that they have no inertia or their inertia is decoupled form the network. To assess the impacts of non-synchronous generations, two non-synchronous penetration (NSP) levels of 14% and 38% are considered. Under 14% renewable
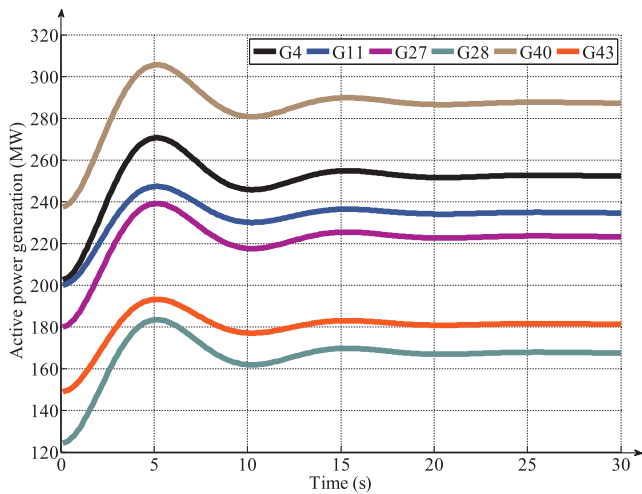
Fig. 7. Active power generation of generators contributing to primary frequency control following sudden outage of G36 at the peak hour.
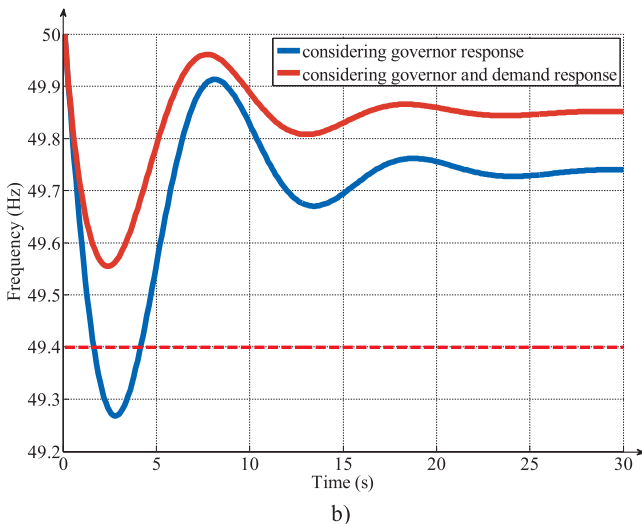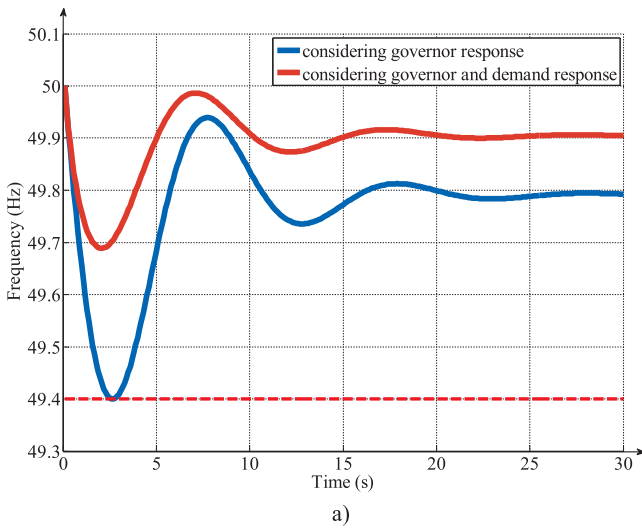
Table 5
System inertia in different NSP levels.

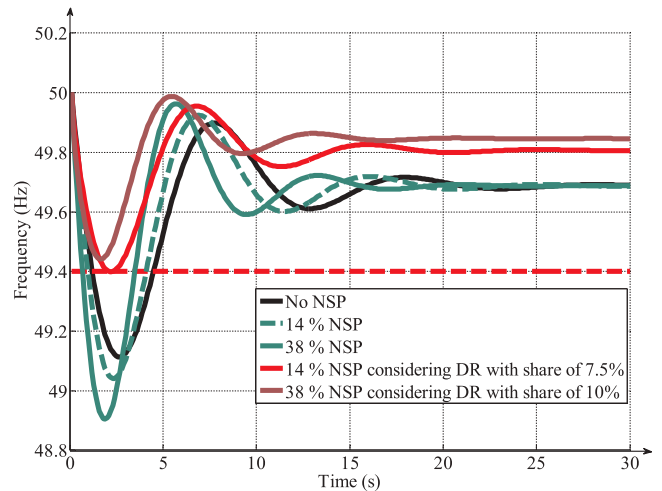| Scenario	Hour	H (sec)
NSP = 0%	8	2.629
	9–10	2.798
	11–13	2.782
NSP = 14%	8	2.117 (19.5% decrease)
	9–10	2.357 (15.8% decrease)
	11–13	2.387 (14.2% decrease)
NSP = 38%	8	1.460 (44.5% decrease)
	9–10	1.792 (35.9% decrease)
	11–13	1.881 (32.4% decrease)

Fig. 9. Contributions of smart loads in inertial frequency response under renewable non-synchronous penetration.
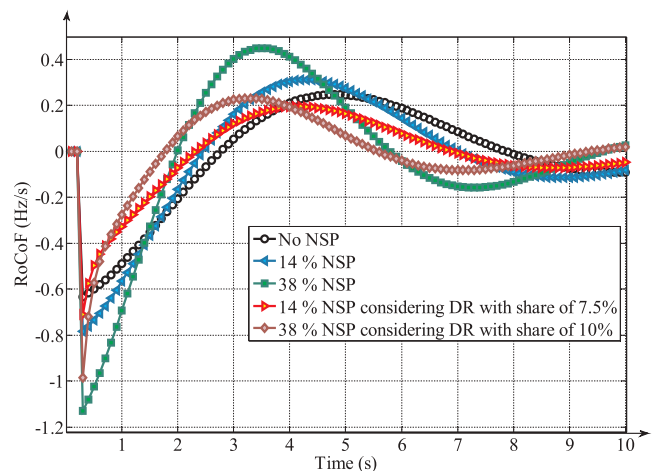

a)

Fig. 10. Effect of smart loads in RoCoF reduction under renewable non-synchronous penetration scenario.

b)

Fig. 8. Post-contingency frequency response for the (a) worst N-1 contingency (i.e. G36) and (b) an N-2 contingency (i.e. G36 and G37) at the peak hour.

penetration, generators G30, G34, G35, G37, G53, and G54 are replaced with free-inertia power plants (i.e. wind farms and photovoltaic). Under 38% renewable penetration, generators G5, G10, G29, and G45 are also

replaced with inertia-free resources. The system inertia in all scenarios is given in Table 5. According to Table 5, when the NSP level is increased, the system inertia is decreased considerably. Smart motor loads are considered to improve the system frequency response with time response of 0.2 s. The frequency responses at hour 8, in this case, are depicted in Fig. 9. It can be seen that due to the significantly decreased system inertia, and without considering the smart load the governors fail to prevent the activation of UFLS relays and the frequency nadir falls further. However, the demand response of smart motor loads brings the system frequency back to its permissible range far from the thresholds of UFLS relays (e.g. frequency nadir is greater
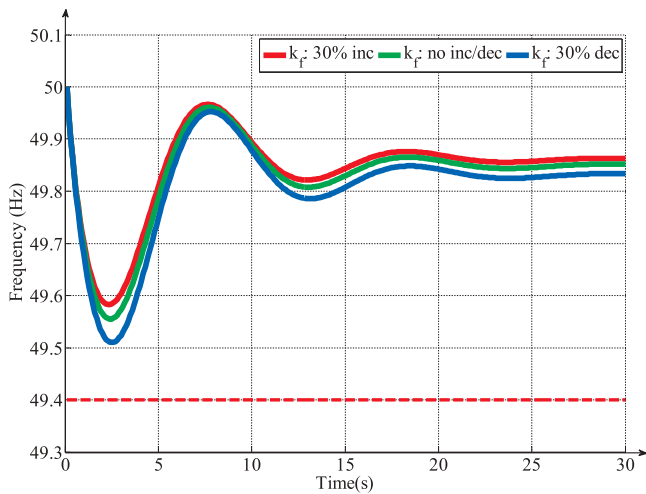
Fig. 11. Sensitivity analysis of system frequency response to frequency dependency parameter of smart loads.
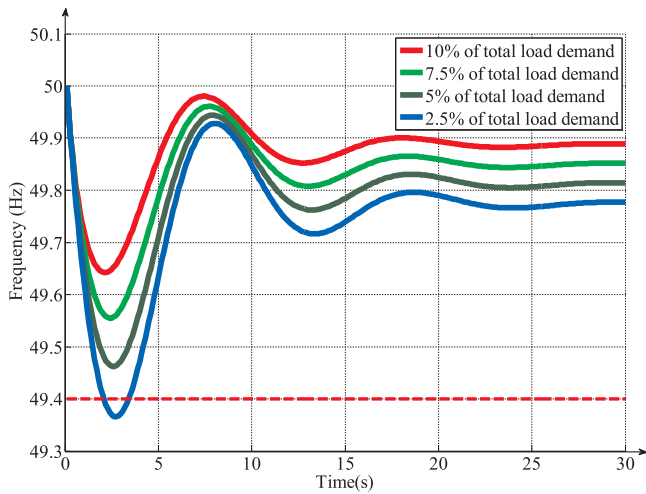

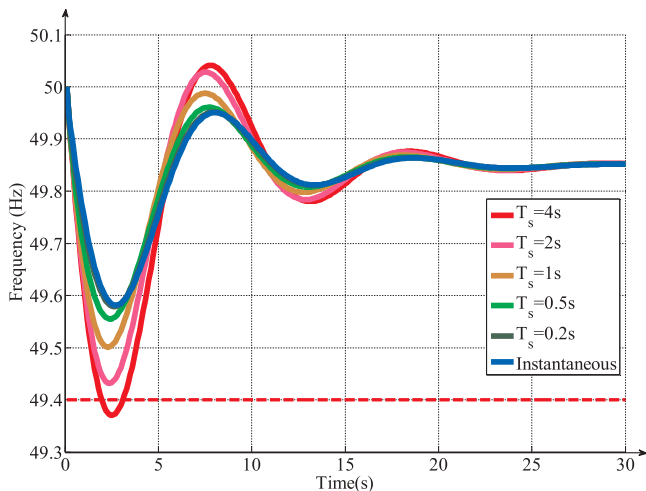**Fig. 12.** Sensitivity analysis of system frequency response to share of responsive drive-connected motor loads.

Fig. 13. Sensitivity analysis of system frequency to time constant of drive.

than 49.4 Hz). In the worst scenario (i.e. 38% NSP), provision of 208.95 MW reserve by smart motor loads satisfies the security of the system without any UFLS action (activation of the first stage of the

assumed UFLS scheme, and hence shedding 10% or in other words 281.934 MW). Also, the impact of non-synchronous penetration and the significance of smart load in smoothing RoCoF variations is shown in Fig. 10. It can be seen that the RoCoF values with 7.5% and 10% share of smart load in low and high NSPs respectively, remain below −1 Hz/ sec in all conditions.

4.4. Case study IV: Impact of smart motor loads

In this case, a sensitivity analysis is carried out to verify the impact of smart loads in system frequency response. Different parameters of smart motor loads including the size of smart loads, the operating and minimum frequency of drive (i.e. $f_{i,m}^{dr}$ and $f_{i,m}^{dr-min}$), and the time constant of its response (i.e. T_s) play important roles in efficient contribution of smart loads to primary system frequency response. In this part, different sensitivity analyses are carried out for these parameters.

1) Frequency sensitivity (k_f): The amount of frequency sensitivity depends on load type. In this regard, the DSCED-FSC model is simulated for 30% variation in k_f. The resulted system frequency responses have been illustrated in Fig. 11. It can be seen that higher frequency sensitivity results in more contribution to system frequency response.

2) Size of smart load: It is evident that the share of smart loads in total loads plays an important role in restoring the system frequency response. Although the share of non-critical smart loads is not significant now, however in the future, the higher share of these loads is expected. Based on Fig. 12, a share of 7.5% present a reasonable contribution to frequency response.

3) Time constant of motor drive (T_s): The smart motor loads deliver the primary reserve during a given time constant. In Fig. 13, the resulted system frequency responses under different time constants of smart motor loads have been illustrated. The time constant of smart motor loads has been assumed as $T_s = 0$ s, $T_s = 0.2$ s, $T_s = 0.5$ s, $T_s = 1$s, $T_s = 2$s, and $T_s = 4$ s. It can be seen that for the delayed response, there is a risk of not providing fast enough reserve to arrest frequency excursions. A time constant lower than $T_s = 0.5$ s gives the desired system frequency responses.

5. Discussion

The DSCED-FSC simulations were carried out using a PC with Intel Core i7-3.6 GHz CPU and 32 GB RAM. With a duality gap of 0%, the CPU time for the DED problem considering the frequency stability constraints and neglecting post-contingency security of the system was about 8 s and the CPU time for the DSCED-FSC problem considering all constraints was about 348 s. Most of the nowadays DED schemes have 15Min or 1 h time intervals. In this regard, the proposed method provides reasonable computation effort for the look ahead DSCED-FSC. Note that it is possible to obtain much lower CPU times by using high speed computers and parallel computing, as usually implemented in control centers. The new proposed model for the DED problem considering frequency response was shown to effectively guarantee the system security in post-contingency conditions. In terms of cost, as discussed in the previous section, when considering the frequency stability constraints, the total cost has been increased from 226480.77$ to 227097.90$. Therefore, with a slight increase in the total cost (of 0.27%) the frequency is kept within the safe range in post-contingency conditions. The efficacy of the proposed method depends on the time constants of contributing factors such as governors of generators.

Typical time constants of governors fall in the range of a few seconds to several seconds. Large generators require larger than minutes amount of time to increase or decrease their output power (i.e. they have low ramp up and down rate in normal conditions). However, the governors contribute to system frequency control in emergency ramp rates which are greater than normal ramp rate. In addition, many types of generators such as hydro power plants or gas-turbine units are very fast to increase or decrease their outputs. In our study, we have chosen

a time step of 100 ms for discretizing system frequency response. This time step gives accurate system frequency responses considering some characteristics of frequency response such as frequency nadir. Smaller amounts of this time step pose additional computational burden while does not proportionally increase the accuracy very much. Larger values of discretization time step may result in poor accuracy of the frequency dynamics approximation. We emphasize that this time step corresponds to the differential swing equation of frequency response and hence is not in conflict with the time interval of the algebraic formulation of the main steady state DED. Indeed, the main DED is a look-ahead study and consists of algebraic formulation without any differential equation. All the discretization process is for the system frequency response. The frequency stability issue is modelled as some constraints in the main economic dispatch study. Dynamics of the system frequency is completely governed by the swing equation. Under a given hourly dispatch of active powers, the system frequency response is discretized and solved to check the frequency stability of the power dispatch. In other words, a discretized system frequency response is solved for each hour. Therefore, the algebraic equations of economic dispatch and the equations of the discretized system frequency response are solved simultaneously as a single or integrated optimization model.

Unavoidably, in many power system studies, there is some degree of uncertainty in input parameters such as the availability of smart loads, system inertia and renewable generation. The uncertainties of system parameters have been discussed in [45]. For short term studies such as ED, the level of uncertainties is lower than the uncertainties of long term studies such as power system expansion planning. For this reason, in this study, the uncertainty of input data was neglected.

6. Conclusion and future works

This paper has proposed a short-term look ahead dynamic SCED model considering primary frequency control (DSCED-FSC). It was shown that the conventional DSCED model may not fulfill the frequency stability constraints while the proposed DSCED-FSC model satisfies the frequency safety and thermal limits by a proper generation re-dispatch. It has been shown also that, in addition to conventional primary frequency reserve (e.g. governor actions, inertial response, and natural load damping), the elasticity of smart motor loads, an emerging control option, may contribute to primary frequency reserve significantly, as the activation of first stages of UFLS relays may be avoided. It has been also demonstrated that the time constants of smart motor loads are very important in keeping the frequency nadir greater than a minimum threshold. The major findings of this study are as follows: 1) Neglecting the frequency stability constraints in the economic dispatch may result in frequency instability and UFLS action in case of severe power imbalance, 2) With just a small increase in the total generation cost, a secure dispatch is achieved through the proposed DSCED-FSC method that maintains frequency stability following severe N-1 contingencies, 3) the utilization of the proposed linear AC power flow model allows ensuring the steady state security of the security-constrained economic dispatch problem, 4) Smart loads can efficiently improve the primary frequency response and avoid or postpone any UFLS action in high penetration of non-synchronous generation or under severe contingencies (e.g. double outages or higher). Utilization of other smart loads such as voltage dependent static loads is an open question for further researches. Future work can also be planned to address the renewable generation and smart load uncertainties. Future work is planned to evaluate the contribution of energy storage devices to frequency control and include renewable energy sources uncertainty for SCED in the day-ahead framework.

References

[1] Fu Y, Shahidehpour M, Li Z. Security-constrained unit commitment with AC constraints. IEEE Trans Power Syst 2005;20:1538–50.
[2] Liu Y, Ferris MC, Zhao F. Computational study of security constrained economic dispatch with multi-stage rescheduling. IEEE Trans Power Syst 2015;30:920–9.
[3] Wang Q, Yang A, Wen F, Li J. Risk-based security-constrained economic dispatch in power systems. J Mod Power Syst Clean Energy 2013;1:142–9.
[4] Capitanescu F, Ramos JM, Panciatici P, Kirschen D, Marcolini AM, Platbrood L, et al. State-of-the-art, challenges, and future trends in security constrained optimal power flow. Electr Power Syst Res 2011;81:1731–41.
[5] Han X, Gooi H, Kirschen DS. Dynamic economic dispatch: feasible and optimal solutions. IEEE Trans Power Syst 2001;16:22–8.
[6] Attaviriyanupap P, Kita H, Tanaka E, Hasegawa J. A hybrid EP and SQP for dynamic economic dispatch with nonsmooth fuel cost function. IEEE Trans Power Syst 2002;17:411–6.
[7] Amraee T, Darebaghi MG, Soroudi A, Keane A. Probabilistic under frequency load shedding considering RoCoF relays of distributed generators. IEEE Trans Power Syst 2017.
[8] Pulendran S, Tate JE. Energy storage system control for prevention of transient under-frequency load shedding. IEEE Trans Smart Grid 2017;8:927–36.
[9] Rebours YG, Kirschen DS, Trotignon M, Rossignol S. A survey of frequency and voltage control ancillary services—Part I: Technical features. IEEE Trans Power Syst 2007;22:350–7.
[10] Delille G, Francois B, Malarange G. Dynamic frequency control support by energy storage to reduce the impact of wind and solar generation on isolated power system's inertia. IEEE Trans Sustainable Energy 2012;3:931–9.
[11] Aghamohammadi MR, Abdolahinia H. A new approach for optimal sizing of battery energy storage system for primary frequency control of islanded microgrid. Int J Electr Power Energy Syst 2014;54:325–33.
[12] Morren J, De Haan SW, Kling WL, Ferreira J. Wind turbines emulating inertia and supporting primary frequency control. IEEE Trans Power Syst 2006;21:433–4.
[13] Liu C, Du P. Participation of load resources in day-ahead market to provide primary-frequency response reserve. IEEE Trans Power Syst 2018.
[14] Bhana R, Overbye TJ. The commitment of interruptible load to ensure adequate system primary frequency response. IEEE Trans. Power Syst 2016;31:2055–63.
[15] Dehghanpour K, Afsharnia S. Electrical demand side contribution to frequency control in power systems: a review on technical aspects. Renew Sustain Energy Rev 2015;41:1267–76.
[16] Chakravorty D, Chaudhuri B, Hui SYR. Rapid frequency response from smart loads in great britain power system. IEEE Trans Smart Grid 2017;8:2160–9.
[17] Molina-Garcia A, Bouffard F, Kirschen DS. Decentralized demand-side contribution to primary frequency control. IEEE Trans Power Syst 2011;26:411–9.
[18] Weckx S, D'hulst R, Driesen J. Primary and secondary frequency support by a multi-agent demand control system. IEEE Trans Power Syst 2015;30:1394–404.
[19] Liu J, Zhang W, Liu Y. Primary frequency response from the control of LED lighting loads in commercial buildings. IEEE Trans Smart Grid 2017;8:2880–9.
[20] Restrepo JF, Galiana FD. Unit commitment with primary frequency regulation constraints. IEEE Trans Power Syst 2005;20:1836–42.
[21] Daly P, Flynn D, Cunniffe N. Inertia considerations within unit commitment and economic dispatch for systems with high non-synchronous penetrations, in: PowerTech, 2015 IEEE Eindhoven, 2015, pp. 1–6.
[22] Wen Y, Li W, Huang G, Liu X. Frequency dynamics constrained unit commitment with battery energy storage. IEEE Trans Power Syst 2016;31:5115–25.
[23] Ahmadi H, Ghasemi H. Security-constrained unit commitment with linearized system frequency limit constraints. IEEE Trans Power Syst 2014;29:1536–45.
[24] Chávez H, Baldick R, Sharma S. Governor rate-constrained OPF for primary frequency control adequacy. IEEE Trans Power Syst 2014;29:1473–80.
[25] Lee Y-Y, Baldick R. A frequency-constrained stochastic economic dispatch model. IEEE Trans Power Syst 2013;28:2301–12.
[26] Teymouri F, Amraee T, Saberi H, Capitanescu F. Towards controlled islanding for enhancing power grid resilience considering frequency stability constraints. IEEE Trans Smart Grid 2017.
[27] Carrión M, Dvorkin Y, Pandžić H. Primary frequency response in capacity expansion with energy storage. IEEE Trans Power Syst 2018;33:1824–35.
[28] Cardozo C, van Ackooij W, Capely L. Cutting plane approaches for frequency constrained economic dispatch problems. Electr Power Syst Res 2018;156:54–63.
[29] Darebaghi MG, Amraee T. Dynamic multi-stage under frequency load shedding considering uncertainty of generation loss. IET Gener Transm Distrib 2016;11:3202–9.
[30] Vrakopoulou M, Katsampani M, Margellos K, Lygeros J, Andersson G, Probabilistic security-constrained AC optimal power flow. In: PowerTech (POWERTECH), 2013 IEEE Grenoble; 2013. p. 1–6.
[31] Javadi M, Amraee T. Economic dispatch: a mixed-integer linear model for thermal generating units. In: 2018 IEEE international conference on environment and electrical engineering and 2018 IEEE industrial and commercial power systems Europe (EEEIC/I&CPS Europe); 2018. p. 1–5.
[32] Javadi M, Amraee T. Mixed integer linear formulation for undervoltage load shedding to provide voltage stability. IET Gener Transm Distrib 2018.
[33] Committee PSR. IEEE guide for the application of protective relays used for abnormal frequency load shedding and restoration. IEEE Std C 2007;37:c1–43.
[34] Yu M, Hong SH. A real-time demand-response algorithm for smart grids: a Stackelberg game approach. IEEE Trans Smart Grid 2016;7:879–88.
[35] Shi Q, Li F, Hu Q, Wang Z. Dynamic demand control for system frequency regulation: Concept review, algorithm comparison, and future vision. Electr Power Syst Res 2018;154:75–87.
[36] Kundur P, Balu NJ, Lauby MG. Power system stability and control. New York: McGraw-hill; 1994.
[37] Glover JD, Sarma MS, Overbye T. Power system analysis & design, SI Version: Cengage Learning; 2012.

[38] Samarakoon K, Ekanayake J, Jenkins N. Investigation of domestic load control to provide primary frequency response using smart meters. IEEE Trans Smart Grid 2012;3:282–92.

[39] Drysdale B, Wu J, Jenkins N. Flexible demand in the GB domestic electricity sector in 2030. Appl Energy 2015;139:281–90.

[40] Meng J, Mu Y, Jia H, Wu J, Yu X, Qu B. Dynamic frequency response from electric vehicles considering travelling behavior in the Great Britain power system. Appl Energy 2016;162:966–79.

[41] Wood AJ, Wollenberg BF. Power generation, operation, and control. John Wiley & Sons; 2012.

[42] Anderson PM, Fouad AA. Power system control and stability. John Wiley & Sons; 2008.

[43] G. Optimization, "Inc.,"Gurobi optimizer reference manual," 2015," URL:http://www.gurobi.com; 2014.

[44] Rosenthal RE. GAMS–a user's guide; 2004.

[45] Soroudi A, Amraee T. Decision making under uncertainty in energy systems: State of the art. Renew Sustain Energy Rev 2013;28:376–84.